

Supporting Information

Formation of nitro(so) by-products of concern from the treatment of phenolic compounds by hydroxylamine enhanced Fe(II)/peroxymonosulfate process

Jiebin Duan^{a, b}, Chaoting Guan^{a,*b, c}, Su-yan Pang^d, Jin Jiang^{a, b}.

a. Key Laboratory for City Cluster Environmental Safety and Green Development of the Ministry of Education, School of Ecology, Environment and Resources, Guangdong University of Technology, Guangzhou 510006, China

b. Southern Marine Science and Engineering Guangdong Laboratory (Guangzhou), Guangzhou 511458, Guangdong, China

c. School of Environment and Civil Engineering, Dongguan University of Technology, Dongguan 523106, Guangdong, China

d. Key Laboratory of Songliao Aquatic Environment, Ministry of Education, School of Municipal and Environmental Engineering, Jilin Jianzhu University, Changchun, 130118, China

*Corresponding author: Dr. Chaoting Guan

E-mail: guanct@gdut.edu.cn.

Number of pages:

5 Texts, 11 Figures, 3 Tables

List of Supporting Information.

Text S1. Chemicals.

Text S2. Experimental Procedure.

Text S3. Detailed instrumental and operational parameters for the HPLC/ESI–QqQMS analysis.

Text S4. Determination of PMS by modified iodometric approach.

Text S5. Detection of ROS and $\cdot\text{NO}$ using EPR.

Figure S1. Variation of PMS concentration in Fe(II)/PMS/HA system

Figure S2. Variation of PMSO and PMSO₂ in Fe(II)/PMS/HA system. Conditions: pH 4.0, [PMSO]₀ = 100 μM , [Fe(II)]₀ = 5 - 100 μM , [PMS]₀ = 150 μM , and [HA]₀ = 150 μM .

Figure S3. Effect of methanol on the degradation of phenol (a), production of *p*-nitrosophenol and nitrophenols (b-c), and the sum of yield of *p*-nitrosophenol and nitrophenols (d) in Fe(II)/PMS/HA system. Experimental conditions: pH 4.0, [phenol]₀ = 50 μM , [Fe(II)]₀ = 10 μM , [PMS]₀ = 150 μM , and [HA]₀ = 150 μM .

Figure S4. Effect of isopropyl alcohol on the degradation of phenol (a), production of *p*-nitrosophenol and nitrophenols (b-c), and the sum of yield of *p*-nitrosophenol and nitrophenols (d) in Fe(II)/PMS/HA system. Experimental conditions: pH 4.0, [phenol]₀ = 50 μM , [Fe(II)]₀ = 10 μM , [PMS]₀ = 150 μM , and [HA]₀ = 150 μM .

Figure S5. Effect of *p*-benzoquinone on the degradation of phenol (a), production of *p*-

nitrosophenol and nitrophenols (b-c), and the sum of yield of *p*-nitrosophenol and nitrophenols (d) in Fe(II)/PMS/HA system. Experimental conditions: pH 4.0, [phenol]₀ = 50 μM, [Fe(II)]₀ = 10 μM, [PMS]₀ = 150 μM, and [HA]₀ = 150 μM.

Figure S6. Variation of ·NO EPR signal intensity with HA dose in Fe(II)/PMS/HA system. Reaction conditions: pH 5.0, [Fe(II)]₀ = 100 μM, [PMS]₀ = 1500 μM, and [HA]₀ = 100 - 6000 μM.

Figure S7. Effect of N-acetyl-L-cysteine (NALC) on the degradation of phenol (a), production of *p*-nitrosophenol and nitrophenols (b-c), and the sum of yield of *p*-nitrosophenol and nitrophenols (d) in Fe(II)/PMS/HA system. Experimental conditions: pH 4.0, [phenol]₀ = 50 μM, [Fe(II)]₀ = 10 μM, [PMS]₀ = 150 μM, and [HA]₀ = 150 μM.

Figure S8. Effect of edaravone on the degradation of phenol (a), production of *p*-nitrosophenol and nitrophenols (b-c), and yield of *p*-nitrosophenol and nitrophenols (d-e) in Fe(II)/PMS/HA system. Experimental conditions: pH 4.0, [phenol]₀ = 50 μM, [Fe(II)]₀ = 10 μM, [PMS]₀ = 150 μM, and [HA]₀ = 150 μM.

Figure S9. Effect of HA initial concentration on the sum of NO₂⁻ and NO₃⁻ concentrations in Fe(II)/PMS/HA system after the reaction.

Figure S10. Oxidation of *p*-NSP and formation of 4-NP in Fe(II)/PMS/HA system

Figure S11. Effect of aeration condition on the degradation of phenol (a), production of *p*-NSP (b), production of NPs, and sum of η(NPs) and η(*p*-NSP) in Fe(II)PMS/HA system. Experimental conditions: pH 4.0, [phenol]₀ = 50 μM, [Fe(II)]₀ = 10 μM, [PMS]₀ = 150 μM, and [HA]₀ = 150 μM.

Figure S12. Total ion chromatogram (TIC) of phenol under ESI negative mode.

Experimental conditions: pH 4.0, [phenol]₀ = 50 μM, [Fe(II)]₀ = 10 μM, [PMS]₀ = 150 μM, and [HA]₀ = 150 μM. Reaction time 1 min.

Figure S13. MS² spectra of the main products of phenol (m/z 122 (a), m/z 138 (b), m/z 154 (c), m/z 185 (d), m/z 109 (e), m/z 214 (f), m/z 243 (g)) under negative mode.

Figure S14. Time-dependent evolution of predominant transformation products of phenol in Fe(II)/PMS/HA system. Experimental conditions: pH 4.0, [phenol]₀ = 50 μM, [Fe(II)]₀ = 10 μM, [PMS]₀ = 150 μM, and [HA]₀ = 150 μM.

Table S1. Concentration of NO₂⁻ and NO₃⁻ (μM) at different initial HA concentration (μM) after the reaction in Fe(II)/PMS/HA system. Conditions: 10 μM Fe(II), 150 μM PMS, 10-600 μM HA, pH 4.0.

Table S2. DO concentration before and after the reaction in various aeration conditions

Table S3. Transformation products of phenol in Fe(II)/PMS/HA system identified by HPLC/ESI-QqQMS. Experimental conditions: pH 4.0, [phenol]₀ = 50 μM, [Fe(II)]₀ = 10 μM, [PMS]₀ = 150 μM, and [HA]₀ = 150 μM.

Text S1. Chemicals.

Phenol, 2-nitrophenol (2-NP), 4-nitrophenol (4-NP), 2,4-dinitrophenol (2,4-DNP), 2,6-dinitrophenol (2,6-DNP), hydroxylamine hydrochloride ($\text{NH}_2\text{OH}\cdot\text{HCl}$), methyl phenyl sulfoxide (PMSO), methyl phenyl sulfone (PMSO_2), 5,5-dimethyl-1-pyrroline N-oxide (DMPO), dimethyl sulfoxide (DMSO), ferrous sulfate heptahydrate ($\text{FeSO}_4\cdot 7\text{H}_2\text{O}$) and PMS (available as Oxone ($\text{KHSO}_5\cdot 0.5\text{KHSO}_4\cdot 0.5\text{K}_2\text{SO}_4$)) were purchased from Sigma-Aldrich. Edaravone (1-phenyl-3-methyl-5-pyrazolone) and N-acetyl-L-cysteine (NALC) were purchased from Shanghai Aladdin biochemical Co., Ltd. Para-nitrosophenol (*p*-NSP) (wetted with 40% water) and iron nitrate nonahydrate ($\text{Fe}(\text{NO}_3)_3\cdot 9\text{H}_2\text{O}$) were purchased from Shanghai Macklin biochemical Co., Ltd. Hydroxylamine sulfate ($\text{NH}_2\text{OH}\cdot 1/2\text{H}_2\text{SO}_4$) was purchased from J&K Chemicals. Methanol and acetic acid of HPLC grade were purchased from Tedia. Diethyldithiocarbamate (DETC) was purchased from Sinopharm Chemical Reagent Co., Ltd. All chemicals were of reagent-grade or higher, and used as received without further purification. All solutions were prepared with deionized water ($18.2\text{ M}\Omega\cdot\text{cm}$) from a Milli-Q purification system (Millipore, Reference). PMS stock solutions were prepared by dissolving Oxone ($2\text{KHSO}_5\cdot \text{KHSO}_4\cdot \text{K}_2\text{SO}_4$) in deionized water and standardized by an ABTS colorimetric method [1].

Text S2. Experimental Procedure.

Batch experiments were conducted in 50 mL glass bottles on a reciprocating shaker at $25\pm 1^\circ\text{C}$. One target compound (phenol or PMSO) and $(\text{NH}_2\text{OH})_2\cdot\text{H}_2\text{SO}_4$ at desired concentrations were added into 30 mL reaction solution beforehand. Reactions were initiated with the simultaneous addition of FeSO_4 and PMS. Acetic buffer (10 mM) and borate buffer (10 mM) were used for pH 3.0 - 6.0 and 7.0, respectively. At specific time intervals, samples were withdrawn and quenched by excess ethylenediamine tetraacetic acid disodium salt (EDTA) and DMSO before analysis by high performance liquid chromatography (HPLC) or HPLC/ESI-QqQMS. For the experiments performed in N_2 or O_2 condition, the solution was aerated with high-purity N_2 or O_2 for 20 min before the reaction started and purged with N_2 or O_2 constantly throughout the reaction.

All the kinetic experiments were conducted in duplicates or triplicates and the mean values with their standard deviations were presented.

Text S3. Detailed instrumental and operational parameters for the HPLC/ESI-QqQMS analysis.

The HPLC/ESI-QqQMS analysis was operated in enhanced product ion (EPI) modes. The gradient mobile phase consisted of acetonitrile/water (A/B) at a flow rate of 0.2 mL/min, which changed linearly from 10/90 to 90/10 in the first 35 min and kept for 15 min, and then returned in 0.1 min to 10/90, and held for 10 min for re-equilibration. Sample injection volume was 10 μ L. A switch valve between the outlet of HPLC column and the inlet of the mass detector was used to divert the HPLC effluent to the waste in the first 2 min to avoid the possible contamination of mass spectrometer. Fragmentation patterns were performed to derive possible molecular structures. Further, the identities of products were determined by comparing the retention time and peak area with authentic standards, if available. The MS parameters were set as follows: source temperature, 500 $^{\circ}$ C; negative ion spray voltage, -4500 V; gas I and II (N_2), 50 arbitrary units; curtain gas, 30 arbitrary units; entrance potential (EP), -10 V; declustering potential (DP), -100 V; collision energy (CE), -30 V; collision cell exit potential (CXP), -13 V. The data acquisition and its analysis were accomplished by Analyst 1.5.2 software (AB Sciex).

Text S4. Determination of PMS by modified iodometric approach.

PMS in Fe(II)/PMS/HA system was quantified spectrometrically using a VarianCary 300 UV–vis spectrometer according to a modified iodometric approach [2]. Particularly, the iodometric approach is based on the spectrophotometric quantification of I_3^- (352 nm) produced via the oxidation of I^- by an oxidant in the presence of excess I^- . In Fe(II)/PMS/HA system, HA could reduce I_3^- to I^- obviously in neutral and alkaline conditions, which interferes with the determination of PMS by iodometric approach. However, the reaction between HA and I_3^- is inhibited significantly under strong acid condition (below pH 2.0) [3]. Therefore, a modified iodometric approach, in which samples withdrawn at specified time intervals are added into the strong acidic KI solution (pH = 2.0), is applied for the determination of PMS concentration. The standard curve of absorbance vs the concentration of PMS is made, where the coefficient of absorbance is $28000 \text{ L}\cdot\text{mol}^{-1}\text{cm}^{-1}$.

Text S5. Detection of ROS and $\cdot\text{NO}$ using EPR

EPR experiments were conducted at room temperature and the spectra were recorded at a Bruker EMX-plus EPR spectrometer. The spin-trapping agent of ROS ($\text{SO}_4^{\cdot-}$, $\cdot\text{OH}$), DMPO was added into the solution before the reaction started and mixed with reaction solution for 15s. The $\cdot\text{NO}$ spin-trapping agent, $(\text{DETC})_2\text{-Fe}^{2+}$ was freshly prepared by mixing DETC and FeSO_4 at a molar ratio of 2:1 [4]. The spin-trapping agent of $(\text{DETC})_2\text{-Fe}^{2+}$ was mixed with reaction solution at 15 s for the identification of $\cdot\text{NO}$. Then, the sample solution was transferred into a capillary tube, which was fixed in the cavity resonator of the EPR spectrometer.

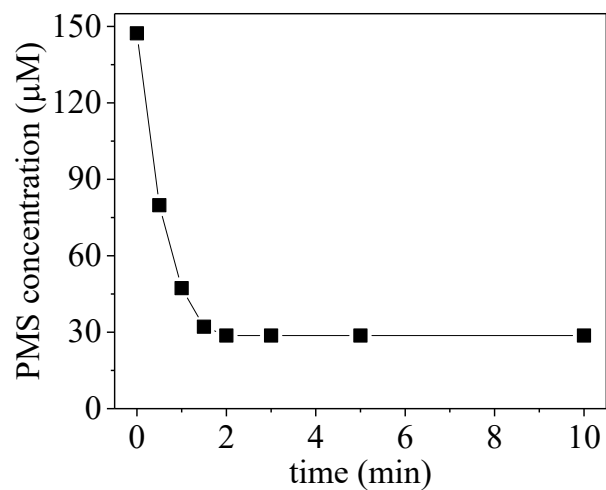


Figure S1. Variation of PMS concentration in Fe(II)/PMS/HA system. Experimental conditions: pH 4.0, $[\text{Fe(II)}]_0 = 10 \mu\text{M}$, $[\text{PMS}]_0 = 150 \mu\text{M}$, and $[\text{HA}]_0 = 150 \mu\text{M}$.

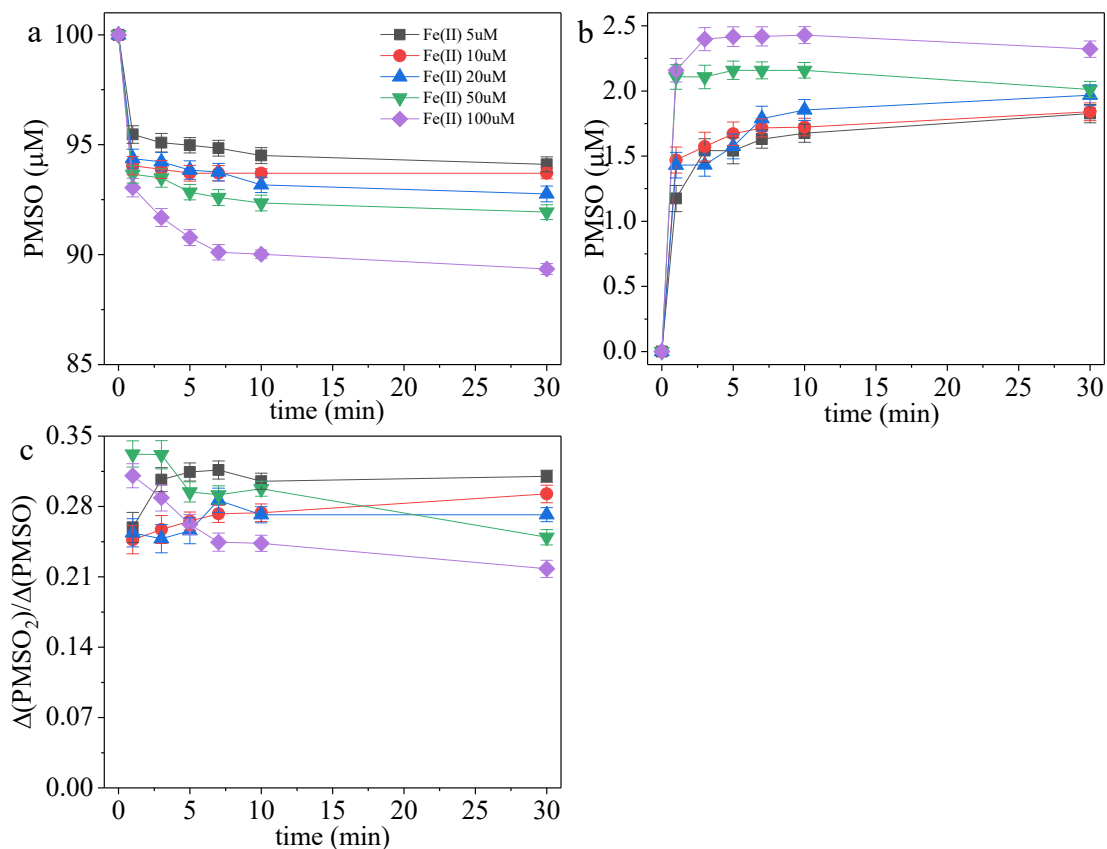


Figure S2. Variation of PMSO and PMSO₂ in Fe(II)/PMS/HA system. Conditions: pH 4.0, [PMSO]₀ = 100 μM, [Fe(II)]₀ = 5 - 100 μM, [PMS]₀ = 150 μM, and [HA]₀ = 150 μM.

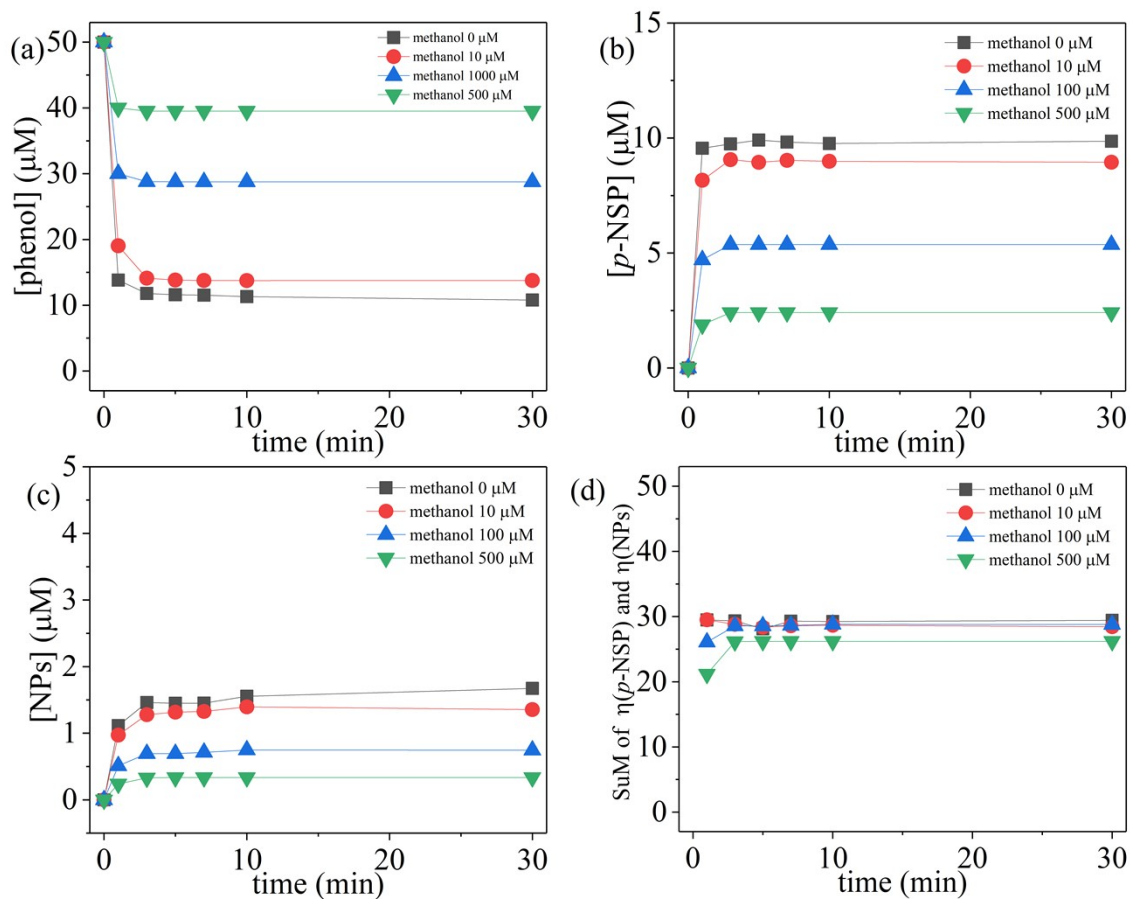


Figure S3. Effect of methanol on the degradation of phenol (a), production of *p*-nitrosophenol and nitrophenols (b-c), and the sum of yield of *p*-nitrosophenol and nitrophenols (d) in Fe(II)/PMS/HA system. Experimental conditions: pH 4.0, [phenol]₀ = 50 μM, [Fe(II)]₀ = 10 μM, [PMS]₀ = 150 μM, and [HA]₀ = 150 μM.

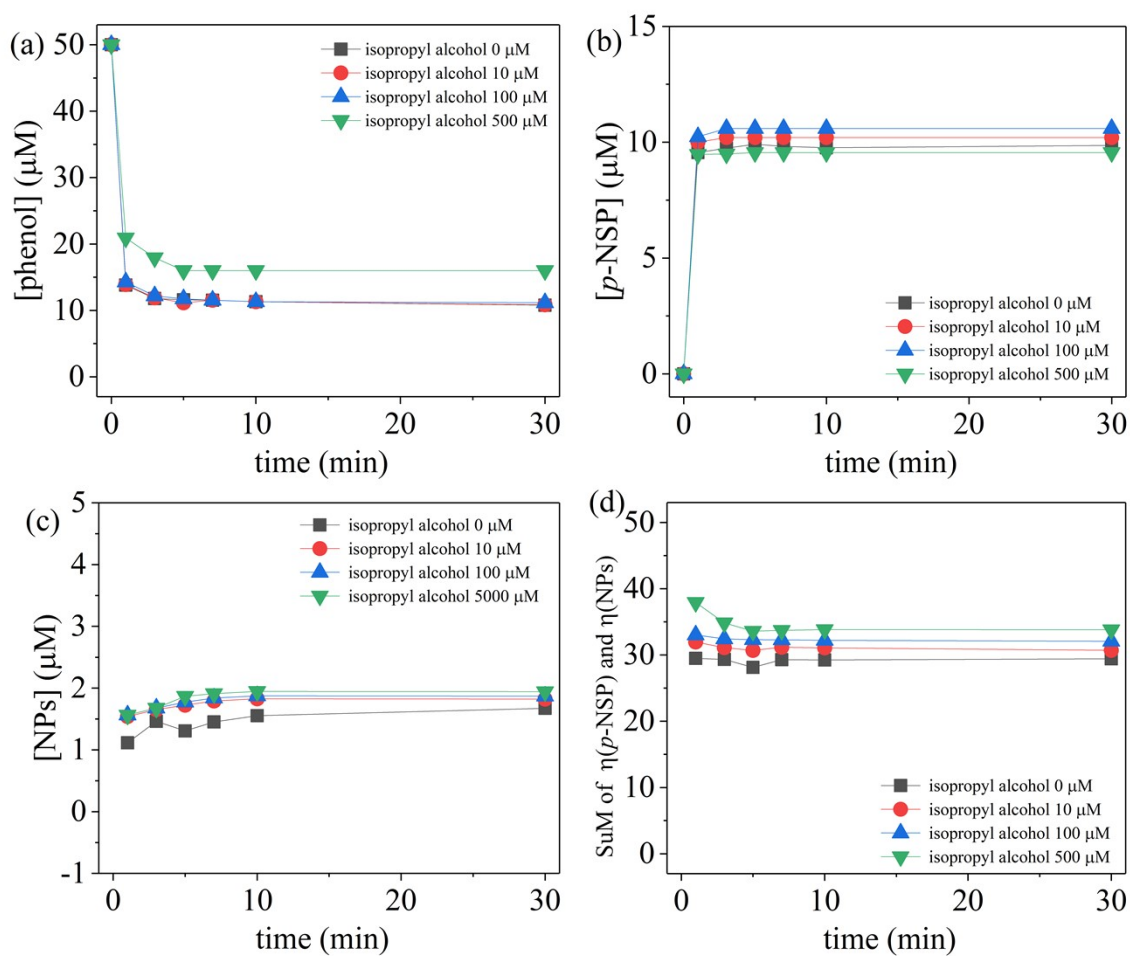


Figure S4. Effect of isopropyl alcohol on the degradation of phenol (a), production of *p*-nitrosophenol and nitrophenols (b-c), and the sum of yield of *p*-nitrosophenol and nitrophenols (d) in Fe(II)/PMS/HA system. Experimental conditions: pH 4.0, [phenol]₀ = 50 μM, [Fe(II)]₀ = 10 μM, [PMS]₀ = 150 μM, and [HA]₀ = 150 μM.

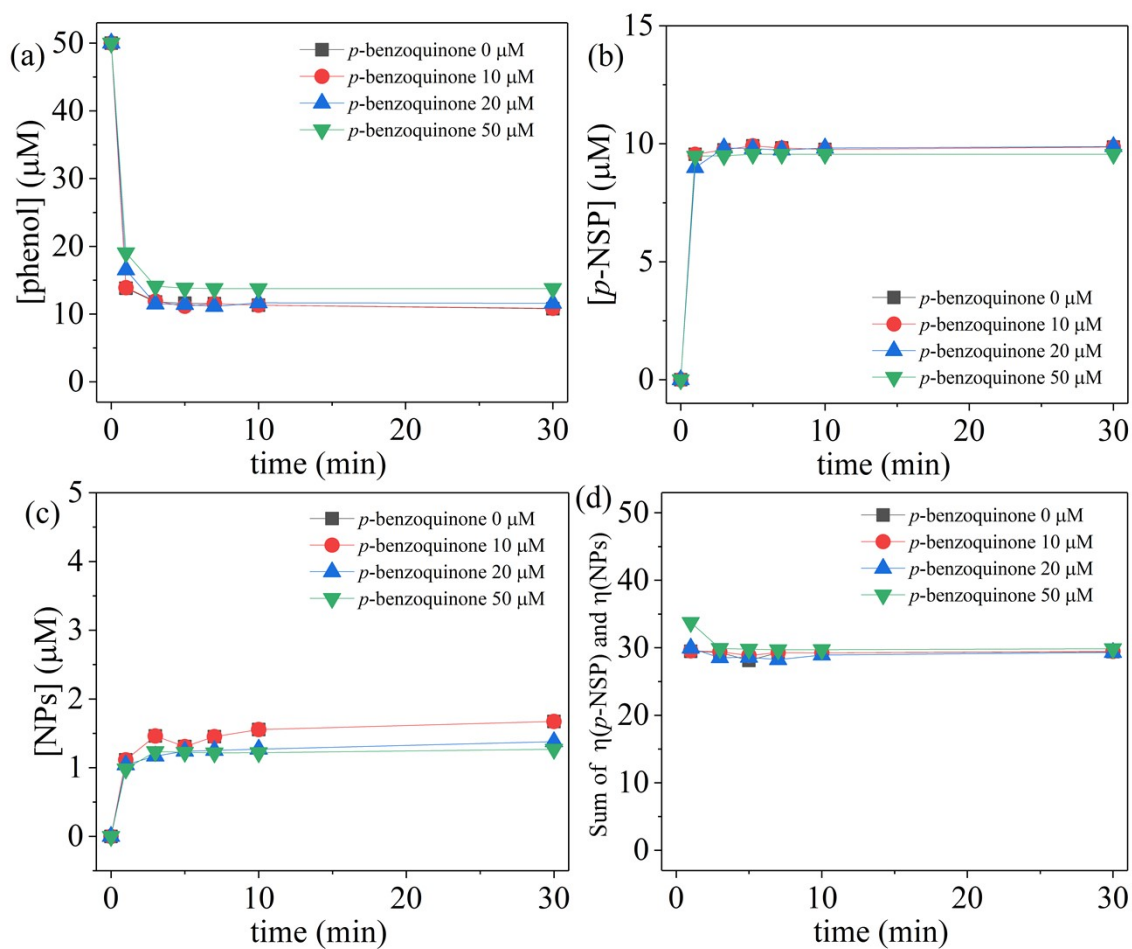


Figure S5. Effect of *p*-benzoquinone on the degradation of phenol (a), production of *p*-nitrosophenol and nitrophenols (b-c), and the sum of yield of *p*-nitrosophenol and nitrophenols (d) in Fe(II)/PMS/HA system. Experimental conditions: pH 4.0, [phenol]₀ = 50 μM, [Fe(II)]₀ = 10 μM, [PMS]₀ = 150 μM, and [HA]₀ = 150 μM.

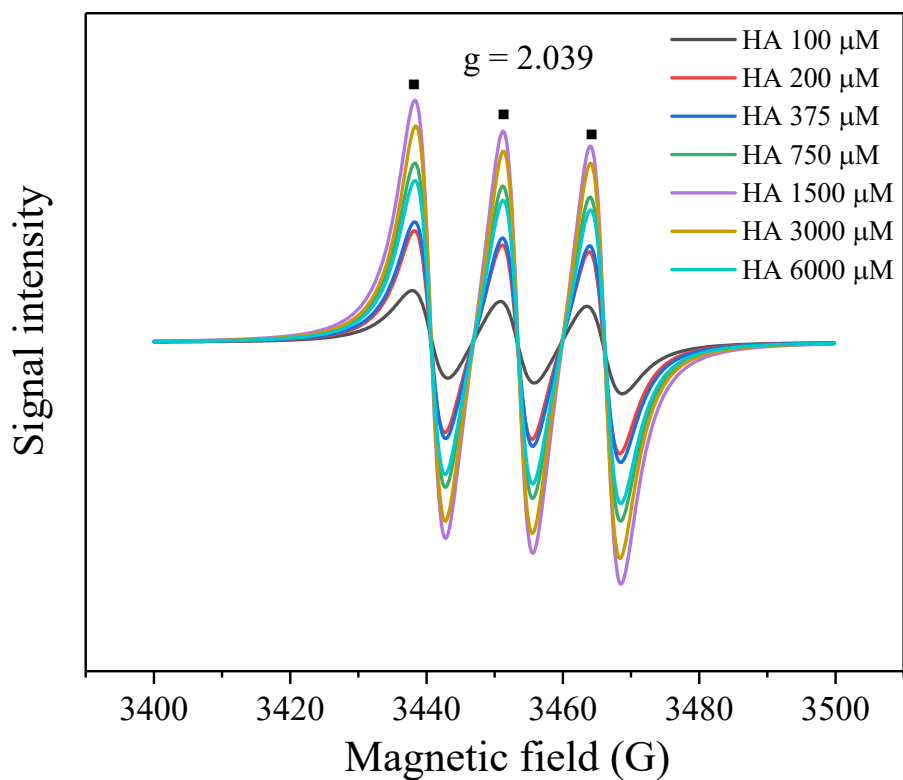


Figure S6. Variation of $\cdot\text{NO}$ EPR signal intensity with HA dose in Fe(II)/PMS/HA system. Reaction conditions: pH 5.0, $[\text{Fe(II)}]_0 = 100 \mu\text{M}$, $[\text{PMS}]_0 = 1500 \mu\text{M}$, and $[\text{HA}]_0 = 100 - 6000 \mu\text{M}$.

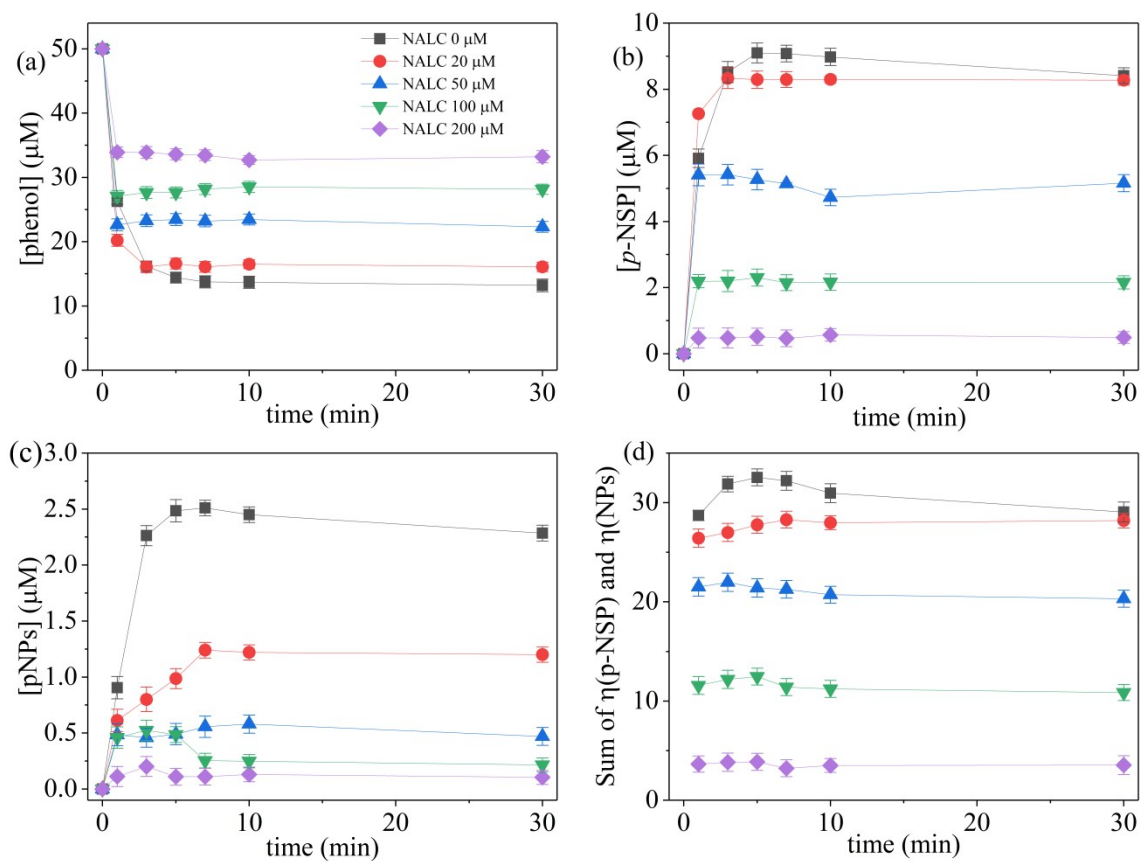


Figure S7. Effect of N-acetyl-L-cysteine (NALC) on the degradation of phenol (a), production of *p*-nitrosophenol and nitrophenols (b-c), and the sum of yield of *p*-nitrosophenol and nitrophenols (d) in Fe(II)/PMS/HA system. Experimental conditions: pH 4.0, [phenol]₀ = 50 μM, [Fe(II)]₀ = 10 μM, [PMS]₀ = 150 μM, and [HA]₀ = 150 μM.

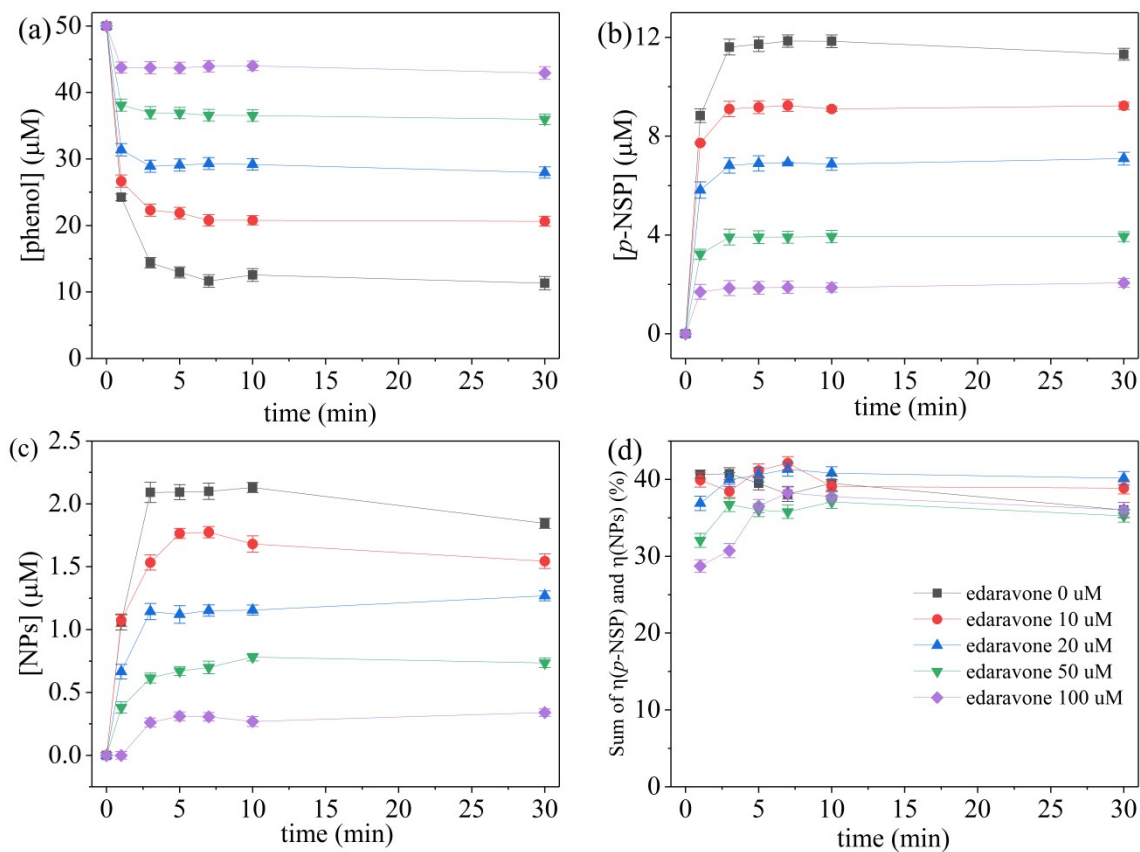


Figure S8. Effect of edaravone on the degradation of phenol (a), production of *p*-nitrosophenol and nitrophenols (b-c), and the sum of yield of *p*-nitrosophenol and nitrophenols (d) in Fe(II)/PMS/HA system. Experimental conditions: pH 4.0, [phenol]₀ = 50 μM, [Fe(II)]₀ = 10 μM, [PMS]₀ = 150 μM, and [HA]₀ = 150 μM.

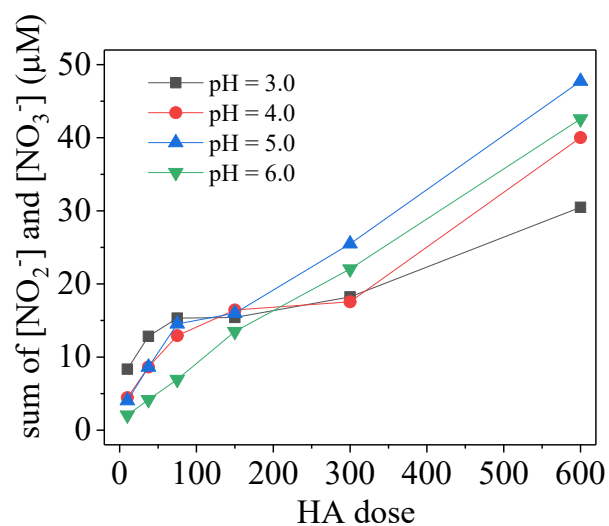


Figure S9. Effect of HA initial concentration on the sum of NO_2^- and NO_3^- concentrations in Fe(II)/PMS/HA system after the reaction. Experimental conditions: pH = 3.0-6.0, $[\text{Fe(II)}]_0 = 10 \mu\text{M}$, $[\text{PMS}]_0 = 150 \mu\text{M}$.

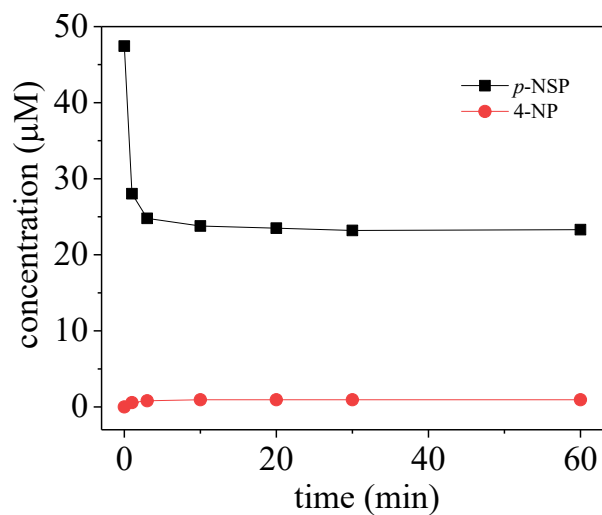


Figure S10. Oxidation of *p*-NSP and formation of 4-NP in Fe(II)/PMS/HA system.

Experimental conditions: pH 4.0, $[p\text{-NSP}]_0 = 47 \mu\text{M}$, $[\text{Fe(II)}]_0 = 10 \mu\text{M}$, $[\text{PMS}]_0 = 150 \mu\text{M}$, and $[\text{HA}]_0 = 150 \mu\text{M}$.

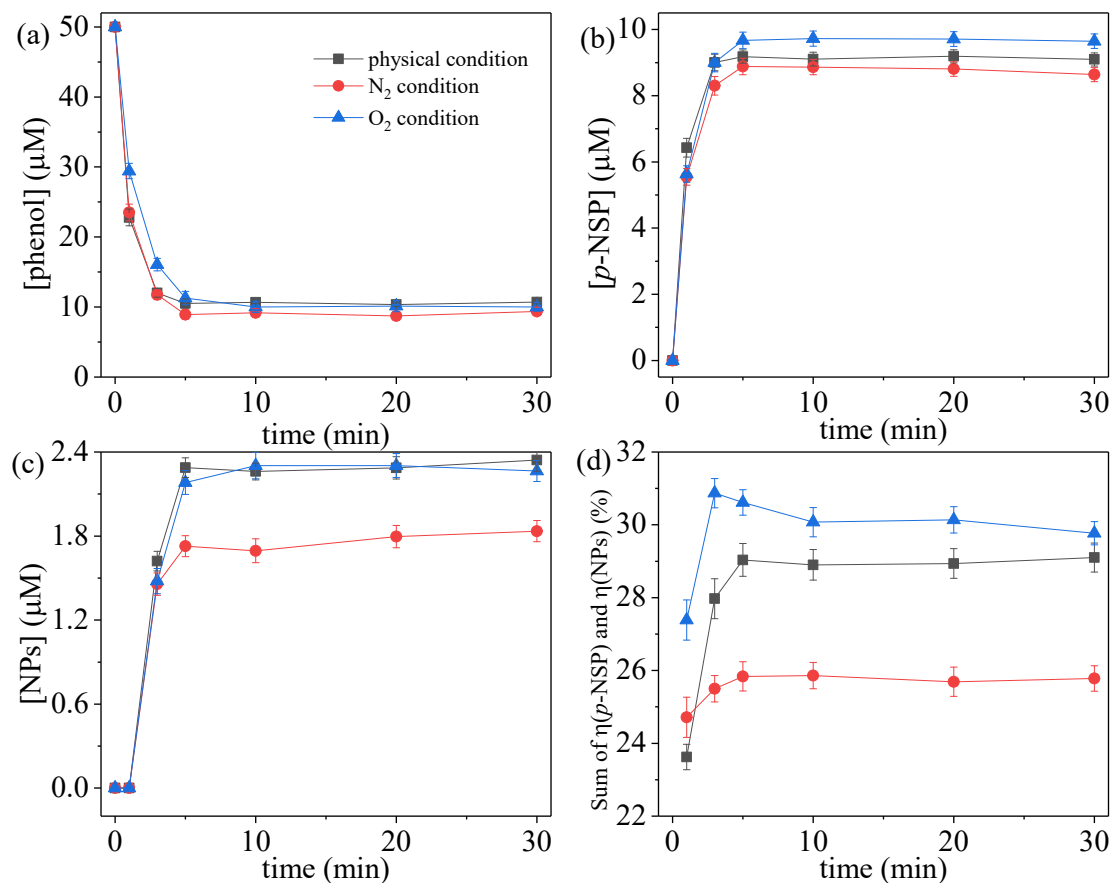


Figure S11. Effect of aeration condition on the degradation of phenol (a), production of *p*-NSP (b), production of NPs, and sum of $\eta(\text{NPs})$ and $\eta(p\text{-NSP})$ in Fe(II)PMS/HA system at pH 4.0. Experimental conditions: $[\text{phenol}]_0 = 50 \mu\text{M}$, $[\text{Fe(II)}]_0 = 10 \mu\text{M}$, $[\text{PMS}]_0 = 150 \mu\text{M}$, and $[\text{HA}]_0 = 150 \mu\text{M}$.

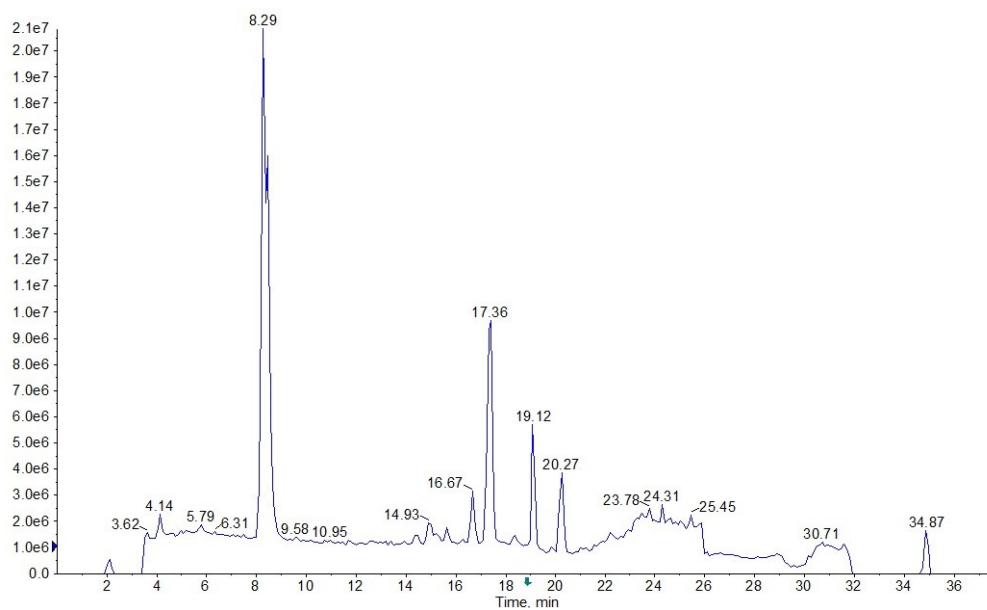
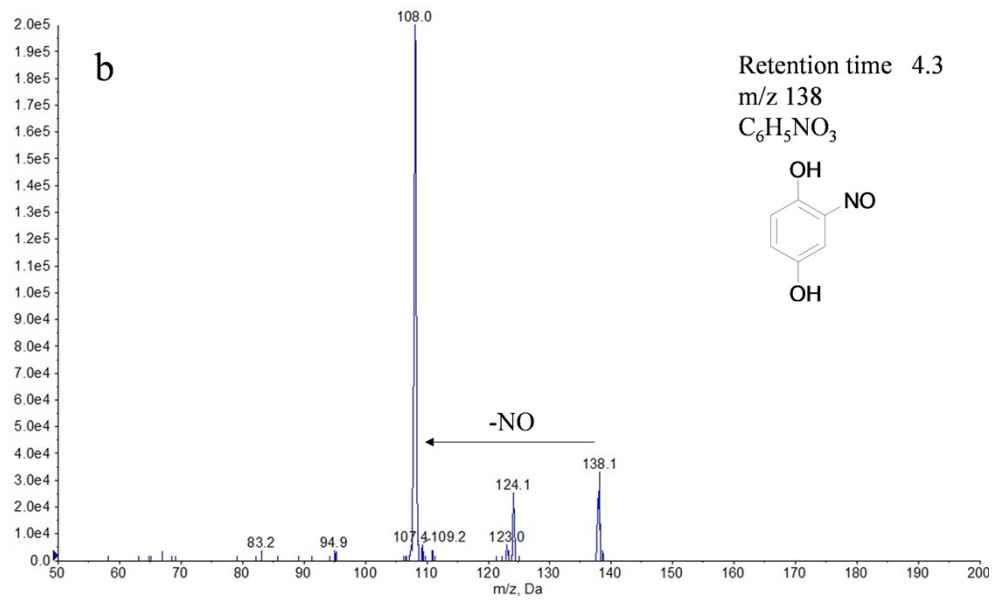
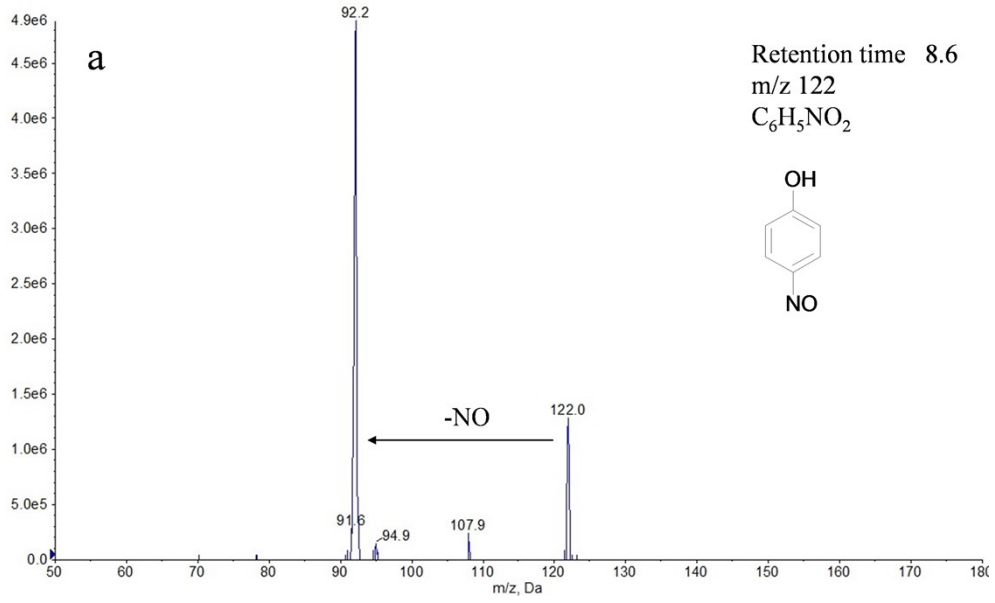
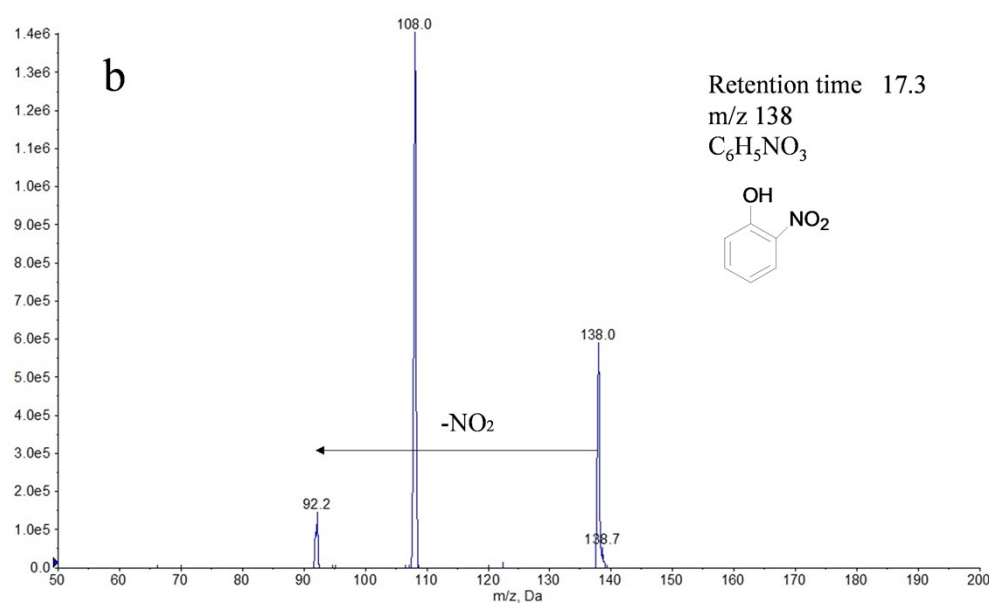
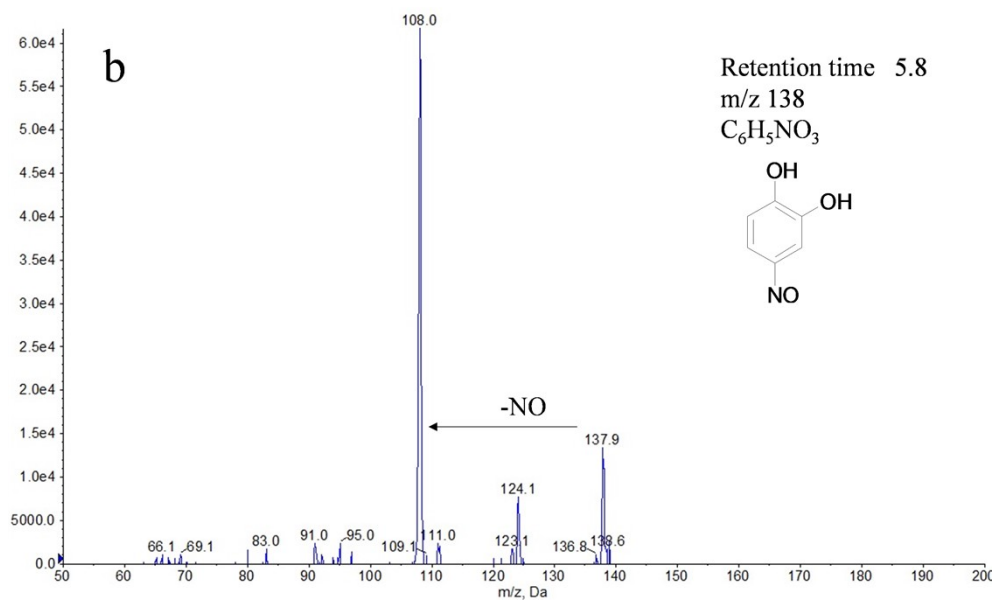
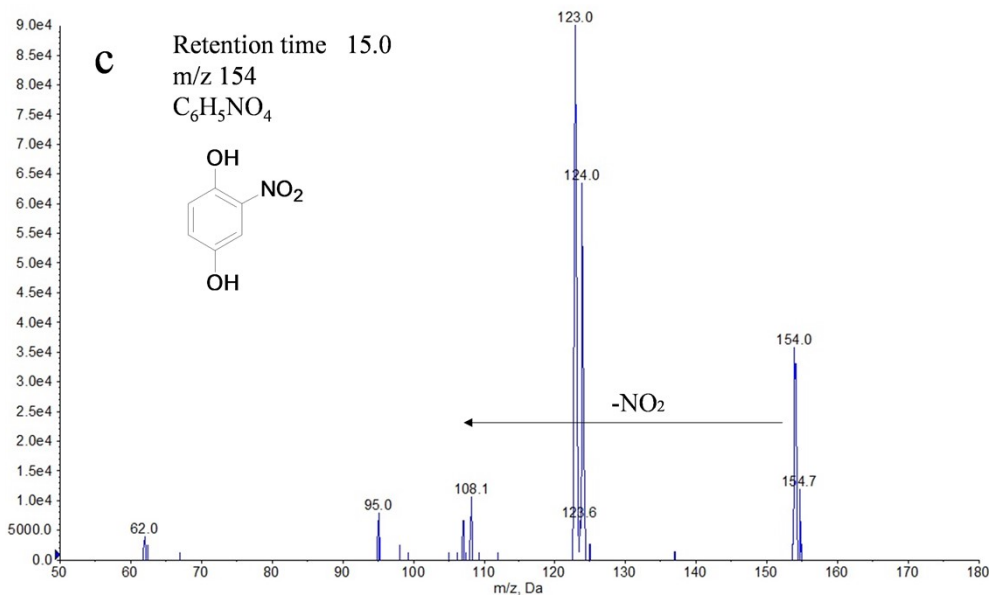
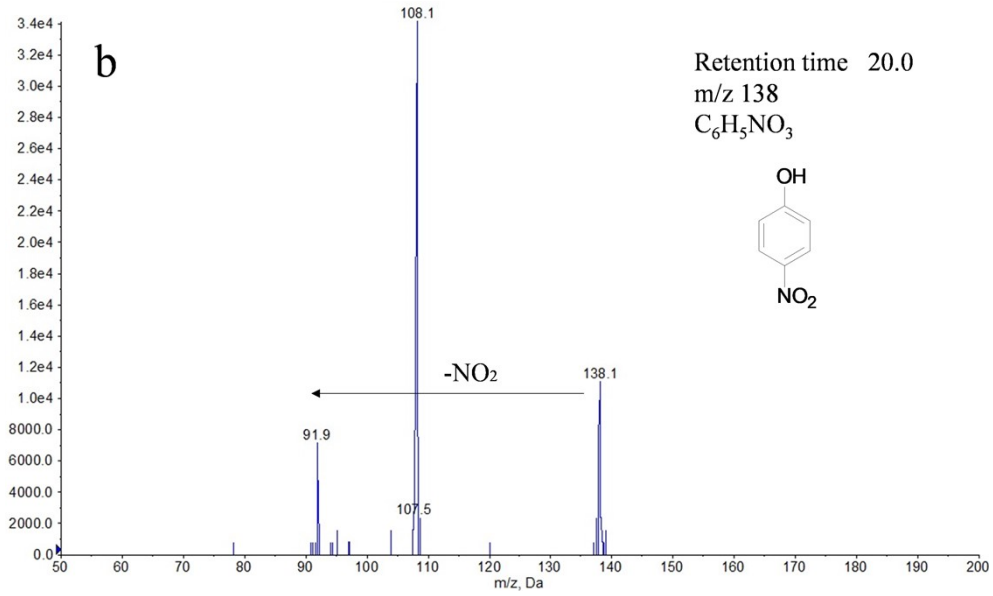


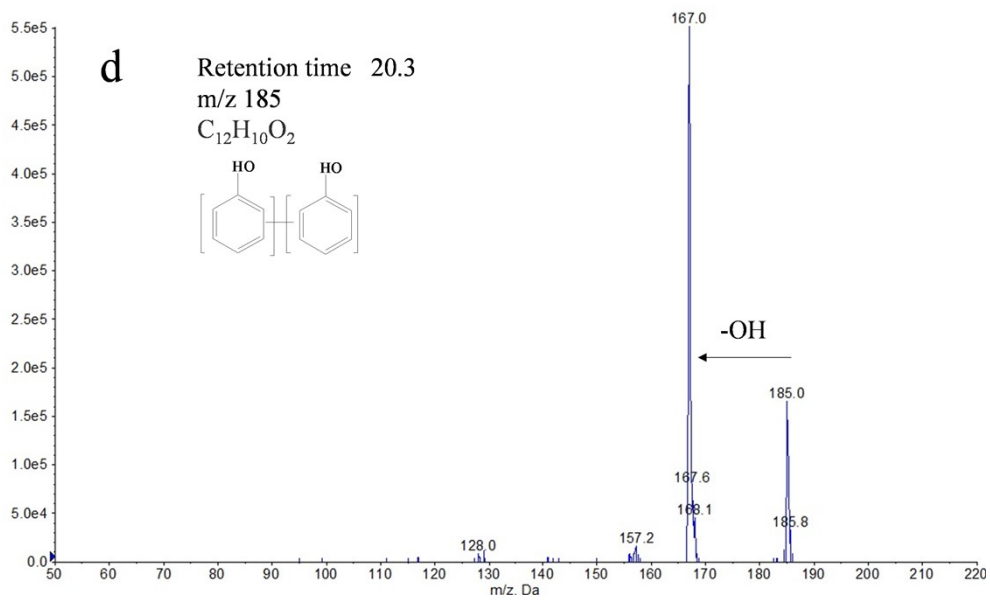
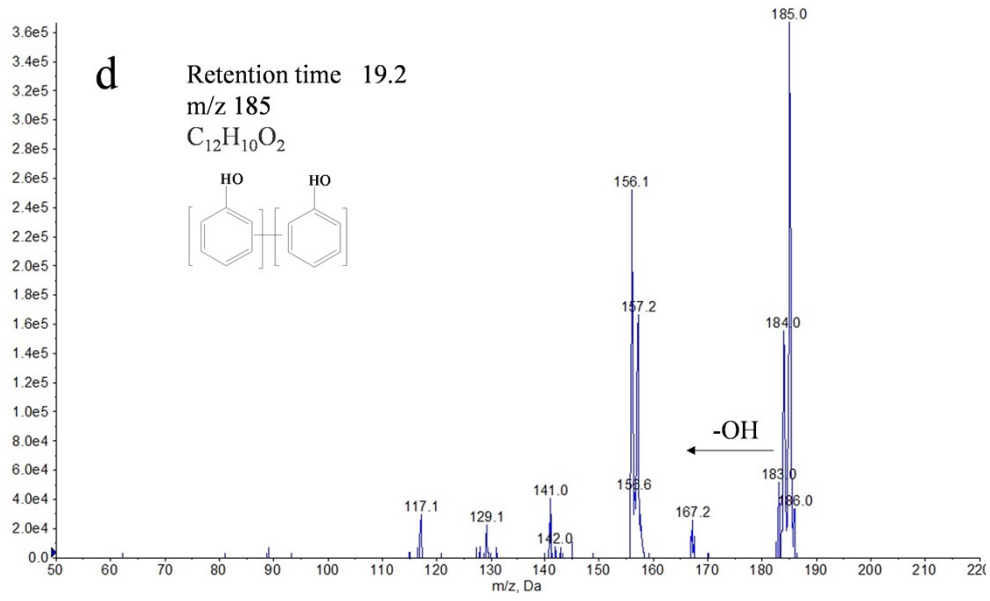
Figure S12. Total ion chromatogram (TIC) of phenol under ESI negative mode.

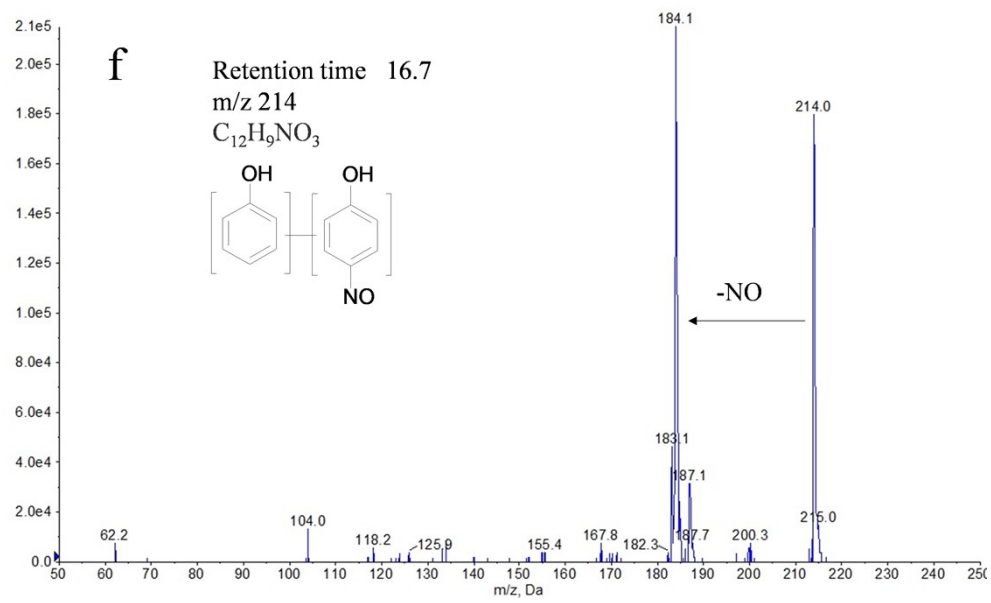
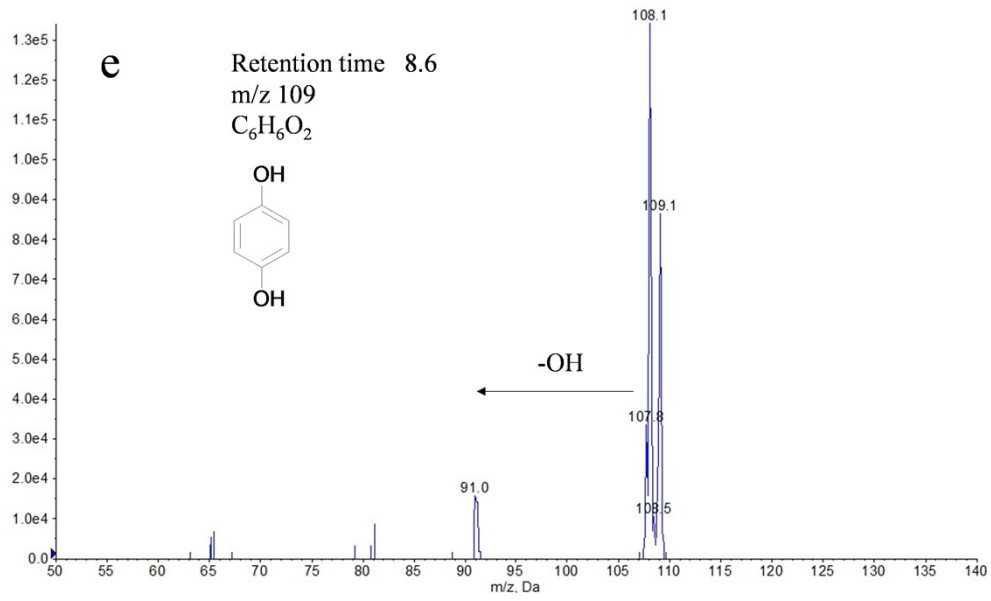
Experimental conditions: pH 4.0, [phenol]₀ = 50 μM, [Fe(II)]₀ = 10 μM, [PMS]₀ = 150 μM, and [HA]₀ = 150 μM. Reaction time 1 min.

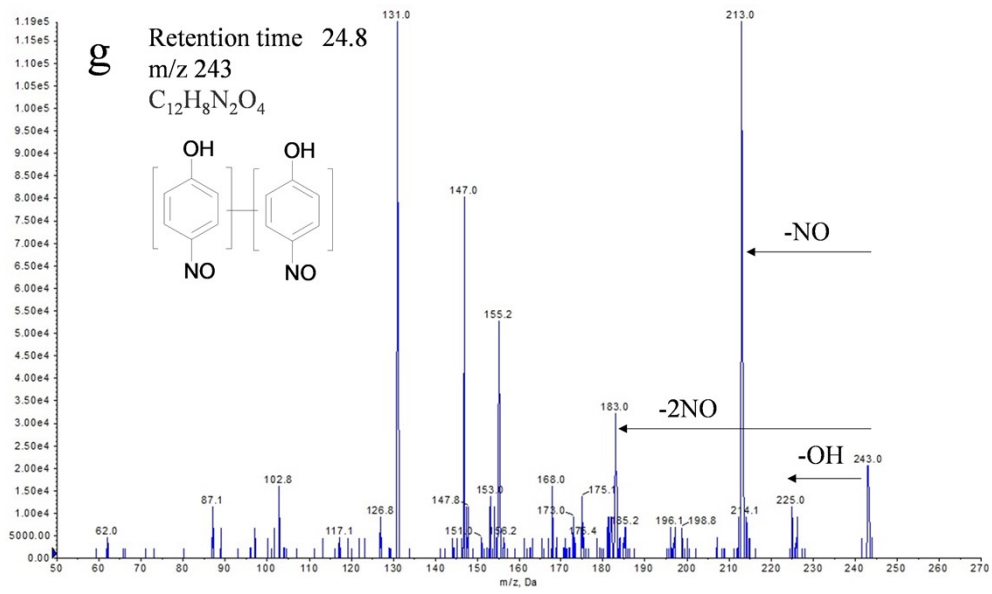
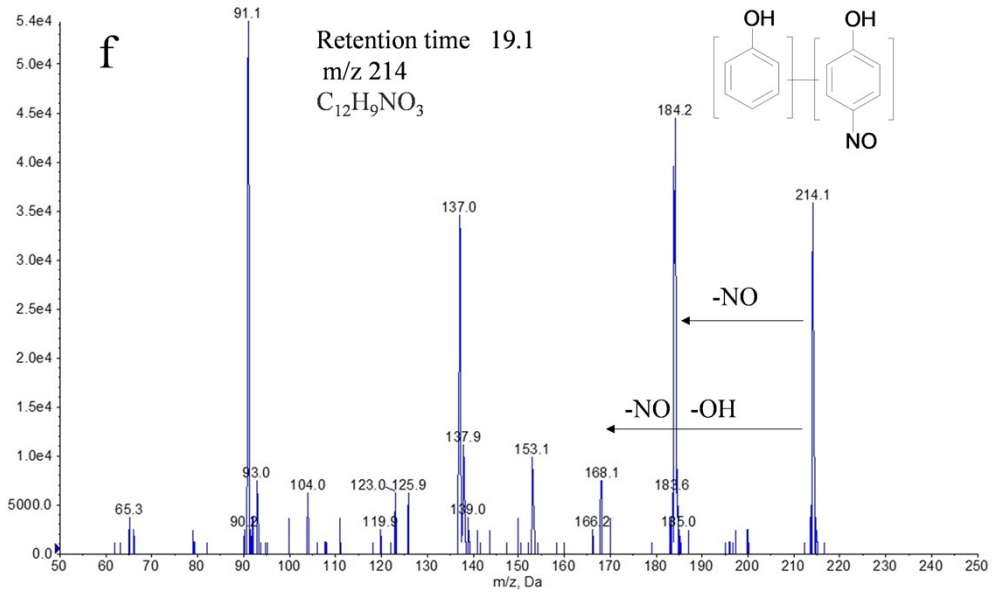












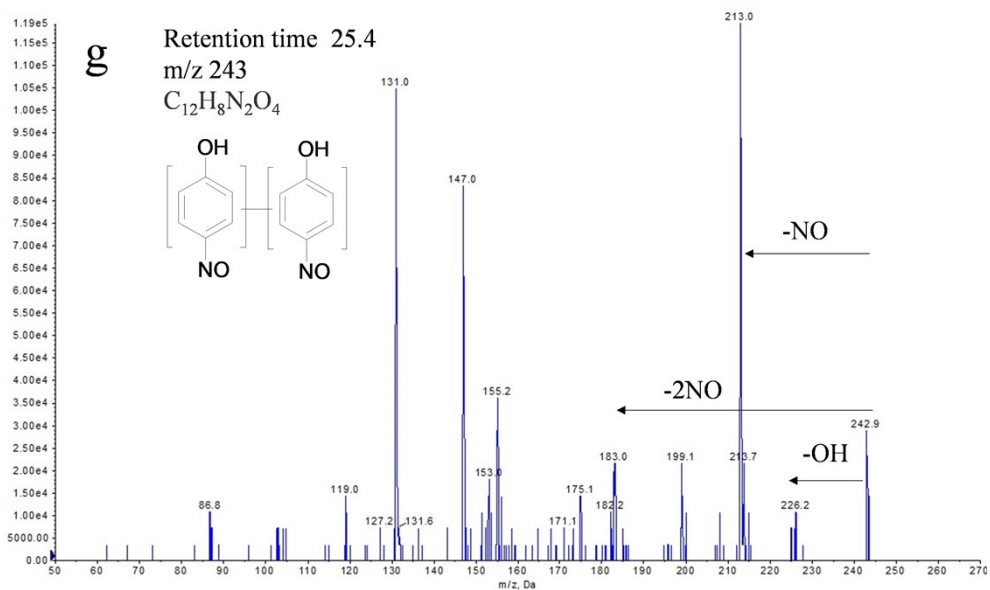
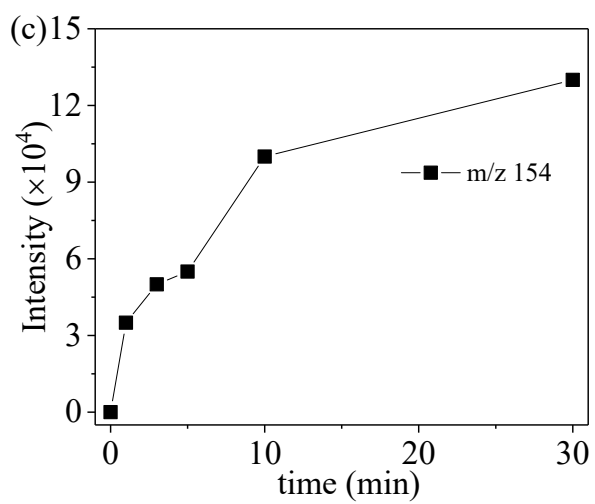
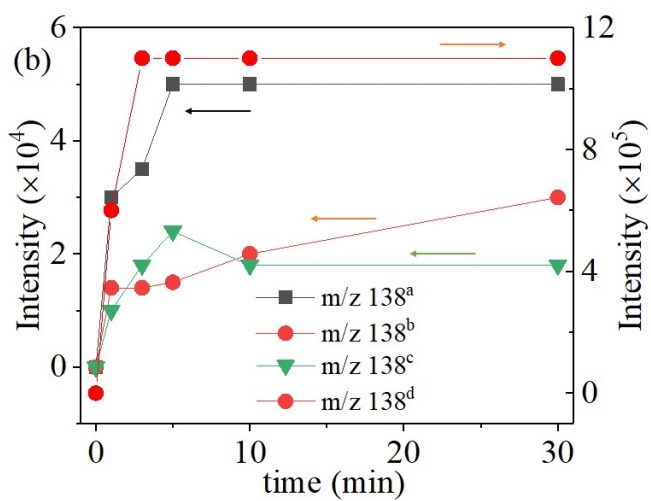
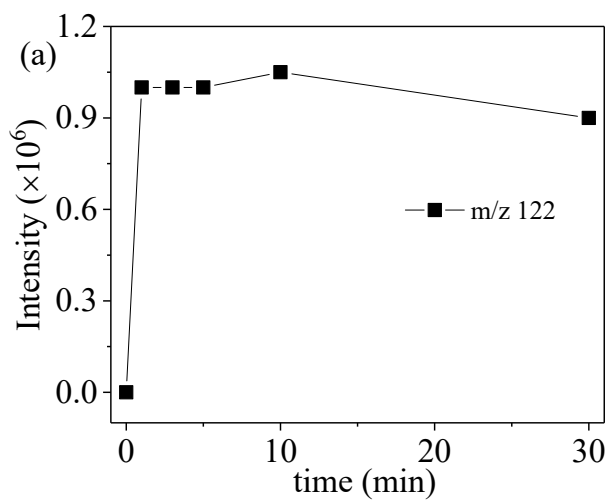
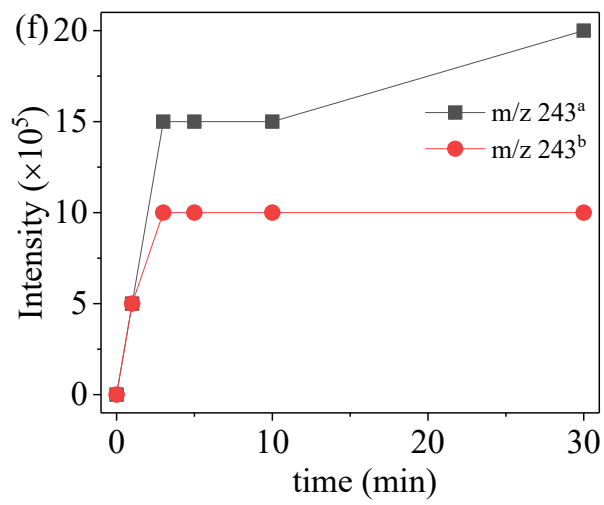
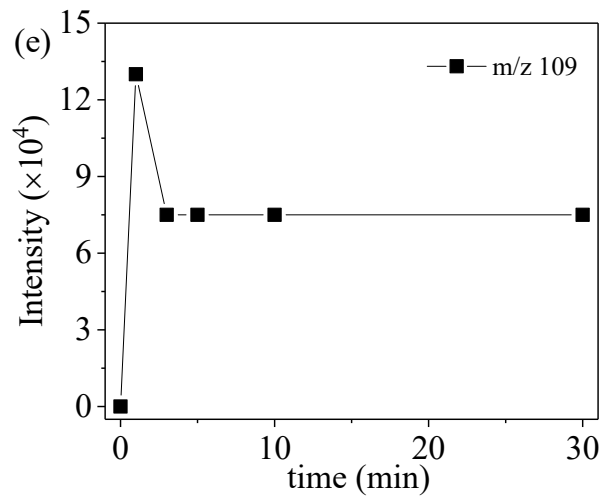
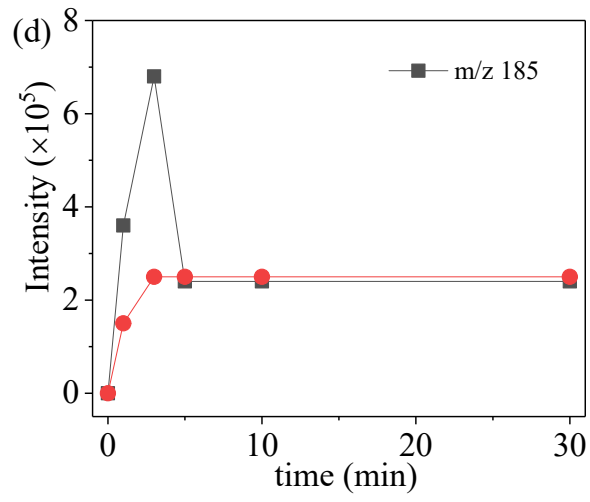


Figure S13. MS² spectra of the main products of phenol (m/z 122 (a), m/z 138 (b), m/z 154 (c), m/z 185 (d), m/z 109 (e), m/z 214 (f), m/z 243 (g)) under negative mode.





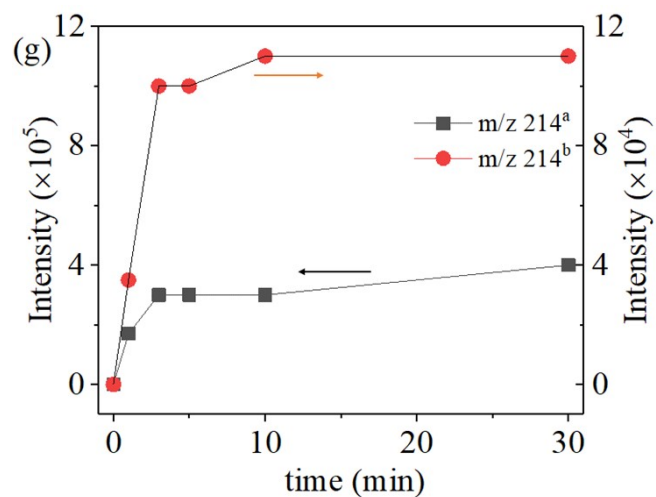


Figure S14. Time-dependent evolution of predominant transformation products of phenol in Fe(II)/PMS/HA system. Experimental conditions: pH 4.0, $[\text{phenol}]_0 = 50 \mu\text{M}$, $[\text{Fe(II)}]_0 = 10 \mu\text{M}$, $[\text{PMS}]_0 = 150 \mu\text{M}$, and $[\text{HA}]_0 = 150 \mu\text{M}$.

Table S1. Concentration of NO_2^- and NO_3^- (μM) at different initial HA concentration (μM) after the reaction in Fe(II)/PMS/HA system. Conditions: 10 μM Fe(II), 150 μM

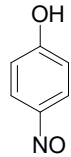
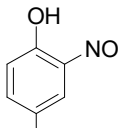
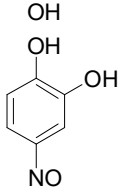
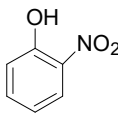
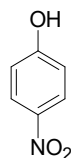
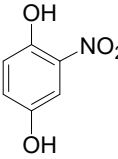
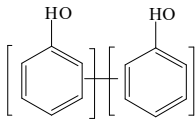
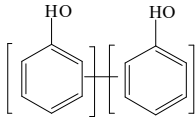
HA	10	20	37.5	75	150	300	600
NO_2^-	0	0	1.1	3.8	6.4	7.2	14.0
NO_3^-	4.4	6.6	7.5	9.2	10.0	10.4	26.1

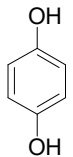
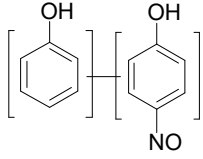
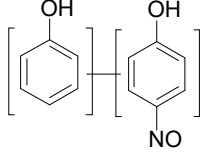
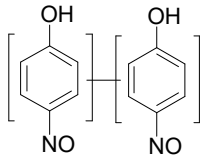
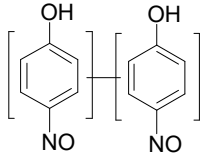
PMS, 10-600 μM HA, pH 4.0.

Table S2. DO concentration (mg/L) before and after the reaction in various aeration conditions.

	N ₂ condition	physical condition	O ₂ condition
0 min	2.05	8.90	32.30
30 min	1.78	8.38	29.59

Table S3. Transformation products of phenol in Fe(II)PMS/HA system identified by HPLC/ESI–QqQMS. Experimental conditions: pH 4.0, [phenol]₀ = 50 μM, [Fe(II)]₀ = 10 μM, [PMS]₀ = 150 μM, and [HA]₀ = 150 μM.

Compound	[M-H] ⁻ m/z	Molecular formula	Proposed chemical structure	Retention time ^a
1	122	C ₆ H ₅ NO ₂		8.6 min
2 ^a	138	C ₆ H ₅ NO ₃		4.3 min
2 ^b	138	C ₆ H ₅ NO ₃		5.8 min
2 ^c	138	C ₆ H ₅ NO ₃		17.3 min
2 ^d	138	C ₆ H ₅ NO ₃		20.0 min
3	154	C ₆ H ₅ NO ₄		15.0 min
4 ^a	185	C ₁₂ H ₁₀ O ₂		19.2 min
4 ^b	185	C ₁₂ H ₁₀ O ₂		20.3 min

5	109	$C_6H_6O_2$		8.6 min
6 ^a	214	$C_{12}H_9NO_3$		16.7 min
6 ^b	214	$C_{12}H_9NO_3$		19.1 min
7 ^a	243	$C_{12}H_8N_2O_4$		25.0 min
7 ^b	243	$C_{12}H_8N_2O_4$		25.4 min

a, b, c, d on the same m/z number represents the isomers of products sharing the same formula.

Reference

1. Yi, Y., Jin, J., Lu, X., Ma, J. and Liu, Y. (2015) Production of Sulfate Radical and Hydroxyl Radical by Reaction of Ozone with Peroxymonosulfate: A Novel Advanced Oxidation Process. *Environmental Science & Technology* 49(12), 7330-7339.
2. Liang C, H.C.F., Mohanty N, et al. , *A rapid spectrophotometric determination of persulfate anion in ISCO*. *Chemosphere*, 2008. **73**(9): p. 1540-1543.
3. Feng Yong, Wu D, Zhou Ying, Shih Kaimin, *A Metal-Free Method of Generating Sulfate Radicals through Direct Interaction of Hydroxylamine and Peroxymonosulfate: Mechanisms, Kinetics, and Implications*. *Chemical Engineering Journal*, 2017.
4. Cao Y. L, G P, Xu Y. C, Zhao, B. L, *Simultaneous detection of NO and ROS by ESR in biological systems*. In *Methods in Enzymology*, Packer, L.; Cadenas, E., ^Eds, 2005. **396**: p. 77-83.